LIMNOLOGY
and
OCEANOGRAPHY LETTERS

ASLO

Open Access

Limnology and Oceanography Letters 2025

doi: 10.1002/lol2.70004

LETTER

Brachiopods as archives of intrannual, annual, and interannual environmental variations

G. Crippa[1*] **H. Jurikova**[2] **M. J. Leng**[3,4] **M. Zanchi**[5,6] **E. M. Harper**[7,8] **J. W. B. Rae**[2] **K. Savickaite**[3] **M. Viaretti**[1] **L. Angiolini**[1]

[1]Department of Earth Sciences, University of Milano, Milan, Italy; [2]School of Earth & Environmental Sciences, University of St Andrews, Fife, UK; [3]National Environmental Isotope Facilities, British Geological Survey, Nottingham, UK; [4]Centre for Environmental Geochemistry, School of Biosciences, University of Nottingham, Loughborough, UK; [5]Center for Complexity and Biosystems, University of Milano, Milan, Italy; [6]Department of Environmental Science and Policy, University of Milano, Milan, Italy; [7]Department of Earth Sciences, University of Cambridge, Cambridge, UK; [8]British Antarctic Survey, Cambridge, UK

Scientific Significance Statement

Given the abundance of brachiopods in the fossil record, their low-magnesium calcite shells that allow higher diagenetic preservation potential, and the possibility to study biomineralization in extant representatives, they have been used to reconstruct ancient ocean conditions. However, limited studies have dealt with sclerochronology because growth lines and increments are not always visible and their periodicity is poorly known. We propose a novel approach applying the Brody–Bertalanffy equation to transform shell length to age, where isotope and elemental data are plotted against the reconstructed ages. We find periodic variations in oxygen isotopes corresponding to annual and intrannual ambient variations in temperate species and interannual variability and endogenous cycles in Antarctic species. This approach can be used to infer Earth's past annual-scale climate and environmental variations.

Abstract

Brachiopods have been employed for environmental and climatic reconstructions in the near and geological past. Traditionally, one datapoint is obtained per shell, providing time-averaged bulk signals. However, brachiopods also have the potential to provide time-resolved information on (sub)annual timescales, but this has been understudied due to difficulties in accounting for brachiopod shell growth. We investigated the distribution of $\delta^{18}O$, $\delta^{13}C$ and Element/Ca along growth profiles of three Recent terebratulides from temperate and polar latitudes. We employed a novel approach using the Brody–Bertalanffy equation to transform shell distances into ages, permitting the study of periodicity in the measured signatures. We show that, superimposed on ontogenetic trends, faster-growing temperate species record annual and intrannual changes at collection sites, whereas slower-growing Antarctic species are also controlled by endogenous cycles. $\delta^{18}O$ profiles reflect annual and

*Correspondence: gaia.crippa@unimi.it

Associate editor: Ming-Tsung Chung

Data Availability Statement: Data and metadata are made available in the Dataverse UNIMI data repository: https://doi.org/10.13130/RD_UNIMI/OQB5LE.

intrannual variations in midlatitudes and interannual variations at high latitudes. $\delta^{13}C$ and Element/Ca are additionally influenced by vital effects.

The shells of rhynchonelliformean brachiopods are hybrid composites of biopolymers and low-Mg calcite with a hierarchical architecture, formed under biological control (Schmahl et al. 2012). The typical shell sequence of extant brachiopods comprises two biomineralized layers: an external primary layer of interdigitating mesocrystals and an inner secondary layer with fibers, and sometimes a tertiary columnar layer (Williams 1968; Williams et al. 1997; Schmahl et al. 2004; Griesshaber et al. 2010; Ye et al. 2018; Simonet Roda et al. 2019). However, many fossil taxa have more complex and varied microstructures (McKinnon 1974; Williams and Cusack 2007; Garbelli et al. 2014; Ye et al. 2020).

Studies of extant and fossil taxa demonstrated that brachiopods precipitate parts (non-specialized secondary and tertiary layers) of their shells in near-equilibrium with seawater, recording geochemical proxy signatures (Carpenter and Lohmann 1995; Parkinson et al. 2005; Brand et al. 2013, 2015; Ullmann et al. 2017; Bajnai et al. 2018; Rollion-Bard et al. 2019; Kocsis et al. 2020; Davies et al. 2023; Rollion-Bard et al. 2024) that are relatively resistant to diagenetic alterations (Lowenstam 1961; Popp et al. 1986; Grossman et al. 1996; Veizer et al. 1999; Angiolini et al. 2009, 2019; Brand et al. 2011; Casella et al. 2018). Brand et al. (2019) showed that oxygen isotopes from the secondary and tertiary layers of modern brachiopod shells maintain a constant offset from abiogenic calcite precipitated in thermodynamic equilibrium by about −1‰: this has been considered as "brachiopod-based equilibrium." The primary layer, however, is out of equilibrium (e.g., Rollion-Bard et al. 2019, 2024).

Brachiopods grow by marginal accretion, generally producing growth increments that enable the study of geochemical variations of accretionary hard tissues (sclerochemistry, Gröcke and Gillikin 2008). Brachiopod sclerochemistry, however, has been only rarely exploited in both fossil (Mii and Grossman 1994; Angiolini et al. 2012; Clark et al. 2016; Roark et al. 2016; Garbelli et al. 2022) and extant brachiopods (Von Allmen et al. 2010; Yamamoto et al. 2011; Takayanagi et al. 2012, 2013, 2015; Butler et al. 2015; Müller et al. 2022). The difficulty in performing sclerochemical studies in brachiopods has mainly been due to the fact that growth increments and lines are frequently not visible within the shell or on its surface, except for limited cases, such as those illustrated by Hiller (1988) and Gaspard (1990).

Sclerochemistry in brachiopods is further complicated by the difficulty of identifying periodicity in growth line formation. Field observations of brachiopod growth rates are not straightforward, with rare direct observations on a monthly or annual timescale (Gaspard et al. 2018), and when grown in aquaria, they do not tend to incorporate seasonal cycles (Jurikova et al. 2020). Brachiopod shell growth can be described by an exponentially decreasing upward function, and it generally conforms to the Brody–Bertalanffy growth model, with growth rates declining during ontogeny (Brey et al. 1995; Peck et al. 1997; Baird et al. 2013). Growth lines may form in response to changes in temperature, food availability, environmental perturbations, or during spawning, and their periodicity shows variable patterns, often species-specific (e.g., Rudwick 1962; Curry 1982; Brey et al. 1995; Peck and Brey 1996; Peck et al. 1997; Schumann 2011; *see* S1 Supporting Information). Major growth lines form mostly as a consequence of low temperature and limited food supply, at least in temperate brachiopods (Hiller 1988; Müller et al. 2022).

Here we present a novel approach to interpret sclerochemical profiles of extant brachiopods that could be extended to fossil shells. It involves the reconstruction of the brachiopod growth curve by applying a Brody–Bertalanffy model that assigns ages to measurements along the longitudinal axis of the shell based on its distance from the umbo, instead of using growth lines. Isotope and elemental data are plotted against the reconstructed ages to obtain time series, which allow the study of potential intrannual and interannual variations.

Materials and methods

Seven specimens belonging to *Gryphus vitreus*, *Liothyrella neozelanica*, and *Liothyrella uva*, coming from different geographic areas, were analyzed in this study (Fig. 1; Table 1). Shells were cut along the maximum growth axis, obtaining a slice 1 cm wide. The primary layer was removed using SiC paper and etching with 5% HCl for 3–5 s. In *G. vitreus* #7, the secondary layer was removed using the same procedure to isolate the tertiary layer. We then performed a high-resolution incremental sampling, collecting powders (∼ 3 mg) through shell abrasion (∼ every 1 mm) with a steel nail file following growth lines.

Shell sections were investigated for their microstructure using a JSM-IT500 (JEOL Ltd, Japan) scanning electron microscope (SEM) at the University of Milan following the procedure of Crippa et al. (2016). Stable isotope analyses were performed at the British Geological Survey, Keyworth (UK) on aliquots ∼ 50–100 μg of carbonate dissolved in 100% H_3PO_4. Oxygen and carbon isotope ratios ($^{13}C/^{12}C$ and $^{18}O/^{16}O$) were measured using an Isoprime dual inlet mass spectrometer plus Multiprep device. Isotope values ($\delta^{13}C$, $\delta^{18}O$) are reported as per mil (‰) deviations of the isotope ratios calculated to the V-PDB scale using a within-run laboratory standard (KCM) calibrated against the international standards (NBS18 and NBS19). Analytical reproducibility was better than 0.09‰ for $\delta^{18}O$ and 0.03‰ for $\delta^{13}C$ (1σ). For each specimen, we calculated the difference between maximum and minimum $\delta^{18}O$ values recorded in the entire shell ($\delta^{18}O$ variation).

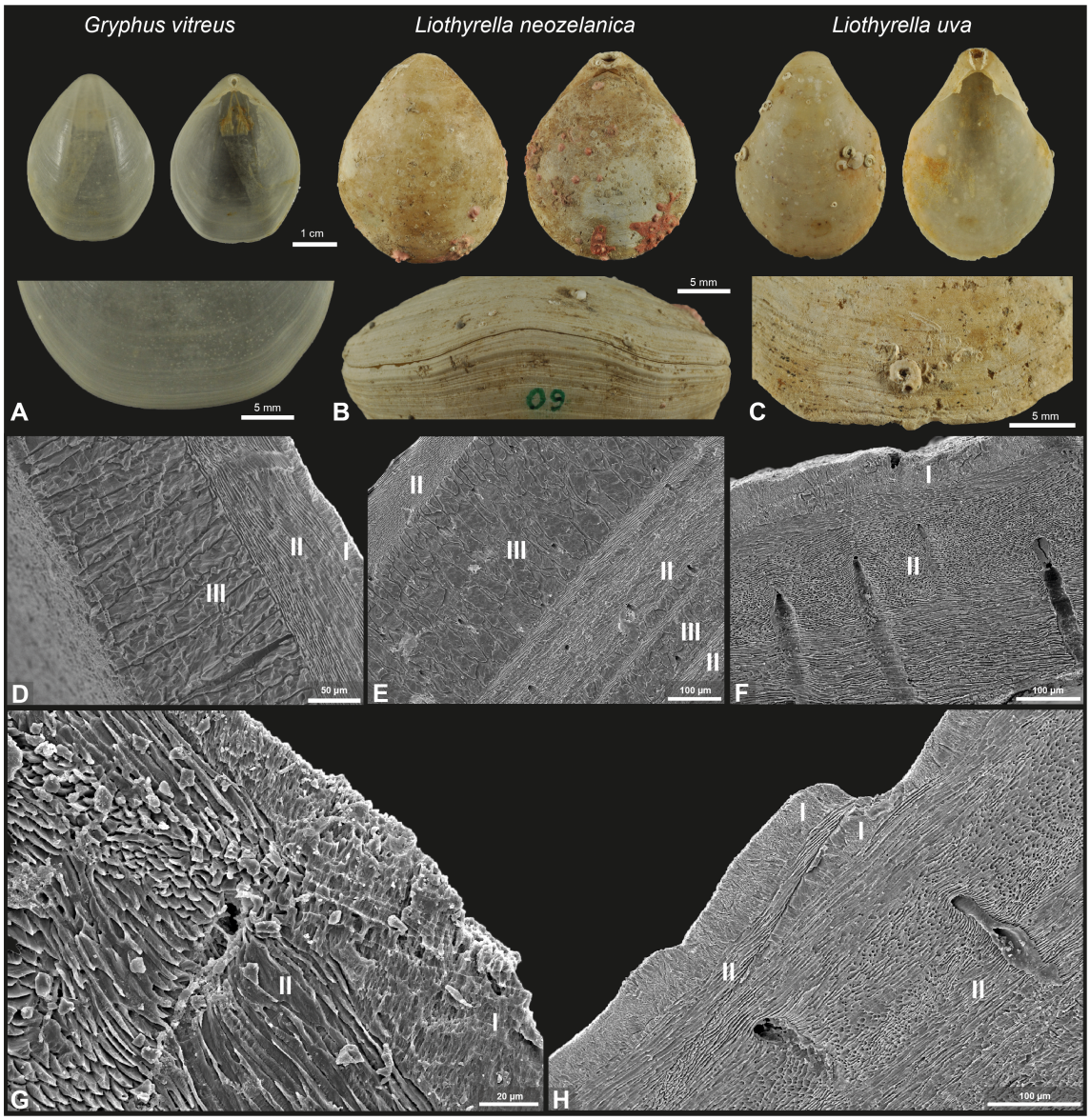

Fig. 1. Specimens of *Gryphus vitreus* (Born, 1778) (#30), *Liothyrella neozelanica* Thomson, 1918 (#67) and *Liothyrella uva* (Broderip, 1833) (#52) analyzed in this study and their shell microstructures at the SEM. Scale bar 1 cm. (**A**–**C**) Growth lines and increments on the shell surface of *Gryphus vitreus* (A, #7, ventral valve, anterior margin), *Liothyrella neozelanica* (B, #60, anterior margin of an articulate specimen) and *Liothyrella uva* (C, #43, ventral valve, anterior margin). (**D**) Three-layer shell of *G. vitreus* #5, showing the dendritic primary, fibrous secondary and columnar tertiary layers regularly sequenced. (**E**) Three-layer shell of *L. neozelanica* #67, showing the irregular alternations of fibrous secondary and columnar tertiary layer. (**F**) Two-layer shell of *L. uva* #52, showing the dendritic primary and fibrous secondary layer. (**G**) Growth lines appearing as weak interruptions of the primary layer, slightly crossing also the secondary layer in *L. neozelanica* #67. (**H**) Growth lines in the anterior part of the shell of *L. uva* #52 crossing also the secondary layer, which forms a wedge of calcite fibers overlapping a newly formed primary layer, which is thus duplicated. I: primary layer, II: secondary layer, III: tertiary layer. Additional images of shell microstructure are available in Plate S1–S3 Supporting Information.

To assess if brachiopod calcite is precipitated in isotope equilibrium with the surrounding seawater, we calculated the $\delta^{18}O$ equilibrium field with the equations of Brand et al. (2019) and Letulle et al. (2023) for biocarbonate, and with Watkins et al. (2014) for inorganic calcite using temperatures and $\delta^{18}O_{sw}$ at collection sites (Tables 1, S3).

An aliquot of ~ 1 mg of the same carbonate powders was analyzed for Element/Ca (Li, Mg, B, U, Na, Al, Sr, Mn, Ba, Cd) on an Agilent 8900 QQQ-ICP-MS at the University of St Andrews. Prior to analysis, all samples were oxidatively cleaned (*see* Jurikova et al. 2019) and dissolved in 0.5 M HNO_3. The analytical precision based on repeated analyses of

Table 1. List of analyzed species, shell layers, specimen IDs, sites of collection, water depths and temperature, salinity, and $\delta^{18}O$ of the seawater. PL: Primary layer, SL: secondary layer, TL: tertiary layer. Water depths, seawater temperatures, salinities, and $\delta^{18}O_{sw}$ are taken from: [1]Ye et al. (2018), [2]Rollion-Bard et al. (2019), [3]E.U. Copernicus Marine Service Information (https://doi.org/10.48670/moi-00052), [4]Brand et al. (2019), [5]Pierre (1999), [6]Lee et al. (2010), [7]Brand et al. (2013), [8]Cross et al. (2015).

Species	Shell layer	Specimen ID	Locality	Water depth (m)	Temperatures (°C)	Salinity (PSU)	$\delta^{18}O_{sw}$ (‰)
Gryphus vitreus	PL, SL, TL	#5, #7	Montecristo (Italy) 42°26′N, 10°04′E	140–160[1]	13–17[2]	38–39[1,3]	+1.25 to +1.36[4,5]
Liothyrella neozelanica	PL, SL, TL	#56, #60, #67	Doubtful Sound (New Zealand) 45°20′S, 167°02′E	18[1]	11.2–17.4[6]	34–35[1,7]	+0.3[4]
Liothyrella uva	PL, SL	#52, #58	Trolval Island, Rothera (Antarctica) 67°35.44′S, 68°12.44′W	15–25[8]	−1.8 to 1[8]	32–34[3,8]	−1 to −1.84[7]

in-house standards and NIST RM 8301 (Foram) measured alongside samples was ≤ 3% (2RSD) for all the reported ratios.

An age-frequency distribution was determined by converting the distance of each sample from the umbo (mm) to age (yr) using a rearranged Brody–Bertalanffy equation (Baird et al. 2013):

$$S_t = S_\infty \left(1 - be^{-Kt}\right)$$

where S_t = size at time t, S_∞ = maximum size, b = scaling parameter for size S_0 different from 0 at time 0, K = growth constant, t = age in years.

Distances of samples from the umbo were therefore used as a basis for shell chronology and not growth lines. However, the length of increments between growth lines, measured on the shell surface of 31 specimens with a stereomicroscope (Motic SMZ-171-TLed; Fig. S4), was used to calculate the parameter $K = 0.14$ for *G. vitreus*, applying a least-square fit to the Brody–Bertalanffy equation with a fixed S_∞ through the Python Scipy library (scipy.optimize.curve_fit method). S_∞ was set to 39.9 mm according to Benigni (1985) and Toma et al. (2022). For *L. neozelanica*, we used $K = 0.18$ and $S_\infty = 52.5$ mm as in Baird et al. (2013). For *L. uva*, $K = 0.036$ was calculated with the method described above for *G. vitreus*; the length of the growth increments was determined on two specimens of *L. uva* and the calculated K fits with values previously determined by Peck et al. (1997). L_∞ was set to 60 mm (Peck et al. 1997). Following Ostrow (2004), for all our specimens we considered the scaling parameter $b = 1$, assuming settlement occurred prior to calcification.

Periodicity within isotope signals was assessed using the Lomb-Scargle periodogram (Lomb 1976; Scargle 1982) generating power spectral profiles through the astropy Python library (The Astropy Collaboration et al. 2022). Following Schulz and Mudelsee (2002), significant frequency modes were identified that are not generated by red noise processes. This procedure combines the theoretical spectrum with Monte Carlo simulations of red noise processes modeled as first-order autoregressive processes to derive a confidence curve at the 95% confidence level. The significant frequency modes are the ones exceeding the confidence curve. Figures were plotted using the Python Matplotlib and Seaborn libraries. *See* S2 Supporting Information for detailed method descriptions.

Results

Temperate species

Gryphus vitreus

The analyzed specimens are ~ 14 yr in age based on the Brody–Bertalanffy equation. The shell fabric is three-layered, regularly sequenced; the secondary layer is thinner than the tertiary layer (Fig. 1A, Plate S1). Growth lines occur as weak interruptions of the primary layer (Plate S1E,F); anteriorly, they cross the secondary layer.

The total $\delta^{18}O$ variation (0.77‰, based on average values of all specimens) corresponds to a temperature variation of 3.1°C using the equation of Brand et al. (2019). In the first 8 yr, the lowest $\delta^{18}O$ value is recorded in the second half of each growth year (Figs. 2A1, S6–S8). Periodicity analysis reveals a 1-yr and 0.5-yr $\delta^{18}O$ periodicity (Fig. 2A2).

The $\delta^{13}C$ and Element/Ca, unlike $\delta^{18}O$, show diverging values in juvenile and mature stages. While $\delta^{13}C$ shows a bell-shaped profile (Figs. 2A1, S6–S8), Element/Ca (with the exception of Cd/Ca) shows a U-shaped pattern (Figs. 4, S20, S21). Periodicity analysis reveals $\delta^{13}C$ intrannual periodicity of 0.5 yr (Fig. 2A2).

Liothyrella neozelanica

The analyzed specimens are 10–12 yr in age based on the Brody–Bertalanffy equation.

The shell fabric is three-layered, irregular, with frequent intercalations of secondary and tertiary layers along the growth axis (Fig. 1B, Plate S2). Growth lines are comparable to *G. vitreus*, but less frequent (Fig. 1D).

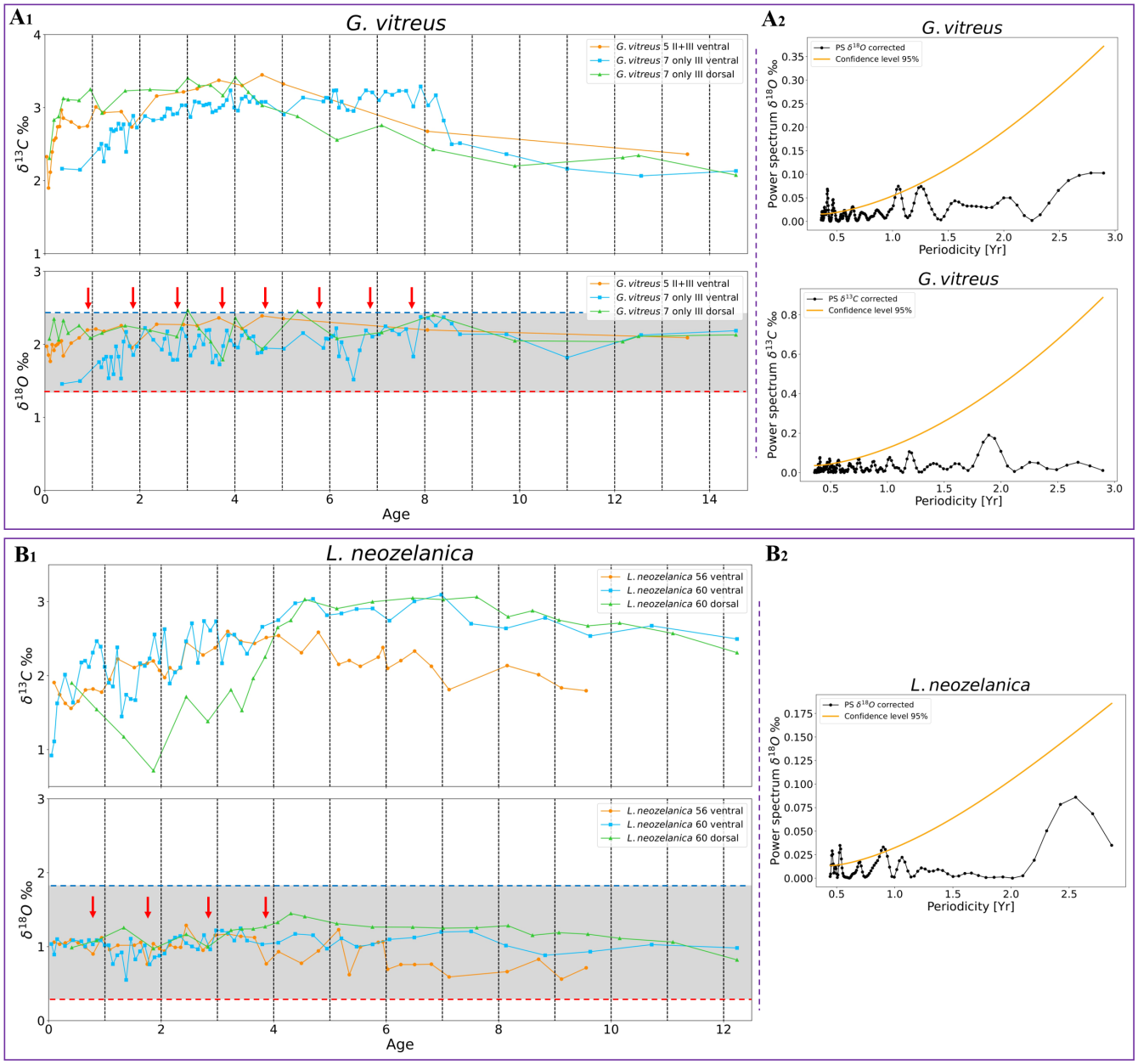

Fig. 2. Time series of $\delta^{13}C$ and $\delta^{18}O$ data of temperate species, *G. vitreus* (**A1**) and *L. neozelanica* (**B1**) obtained by the Brody–Bertalanffy equation with $K = 0.14$ and $S_\infty = 39.9$ mm for *G. vitreus* and $K = 0.18$ and $S_\infty = 52.5$ mm for *L. neozelanica*. For *G. vitreus*, data are plotted for the secondary and tertiary layers sampled together (#5) and for the tertiary layer only (#7); for *L. neozelanica* both layers have been sampled together. The gray horizontal box represents the isotope equilibrium field calculated following Brand et al. (2019) (*see* S2.5 Supporting Information). Red and blue dotted lines delimiting the equilibrium field represent the extremes of the expected range of $\delta^{18}O$ values calculated from the maximum and minimum temperatures at the collection site (red line: lowest $\delta^{18}O$ values, highest temperatures; blue line: highest $\delta^{18}O$ values, lowest temperatures). Red arrows indicate the $\delta^{18}O$ minima recorded in the second half of each growth year. (**A2**, **B2**) The figures describe the power spectrum for the *G. vitreus* data ($\delta^{18}O$ on top, $\delta^{13}C$ on bottom; #7 only tertiary layer, ventral valve) and *L. neozelanica* (only $\delta^{18}O$; #56, ventral valve) respectively, compared with the 95% confidence level curve for red noise; the X-axis represents the periodicity and the Y-axis the power spectrum values. For $\delta^{18}O$ data of *G. vitreus* significant periodicities around 1 and 0.5 yr have been found. For $\delta^{13}C$ data of *G. vitreus* a significant periodicity around 0.5 yr has been found. For $\delta^{18}O$ data of *L. neozelanica* significant periodicities around 1 and 0.5 yr have been found. For $\delta^{13}C$ data of *L. neozelanica* no significant periodicity has been noticed.

The total $\delta^{18}O$ variation (0.68‰) corresponds to a temperature change of 3°C. In juvenile stages, the lowest $\delta^{18}O$ value is often reached in the last part of each growth year (Figs. 2B1, S9–S11). Comparatively less data are available in the mature stages, but the average $\delta^{18}O$ values decrease slightly. Periodicity analysis reveals a 1-yr and 0.5-yr $\delta^{18}O$ periodicity (Fig. 2B2).

Similar to *G. vitreus*, $\delta^{13}C$ values show an overall bell-shaped profile with lower values in the juvenile and mature stages (Figs. 2B1, S9–S11). Periodicity analysis does not reveal a discernible signal. Li, Mg, B, Na, Sr, and to some extent Ba/Ca (Figs. 4A–C,E,G,I, S20, S21) show a shallower U-shaped pattern compared to *G. vitreus*, with higher values recorded in the first years of growth, which decrease afterwards before gradually increasing again anteriorly (except Ba/Ca). Mn/Ca (Fig. 4H) and Cd/Ca (Fig. 4J) show high values in the middle parts of the shell.

Antarctic species

Liothyrella uva

The analyzed specimens are approximately 40 yr in age based on the Brody–Bertalanffy equation. Their shell fabric is two-layered (Fig. 1C, Plate S3). Growth lines occur as in *G. vitreus* (Fig. 1E, Plate S3A,C–E).

The total $\delta^{18}O$ variation (1.58‰) corresponds to a temperature variation of 2.2°C if salinity varies by 2 PSU (Table 1). There is a shift at 12 yr, with a decrease in average $\delta^{18}O$ and $\delta^{13}C$ values (Fig. 3A).

Intrannual patterns are not visible; instead, interannual variations are quite clear with a 1.5- and 3-yr periodicity of both isotope signals and $\delta^{18}O$ maxima corresponding to $\delta^{13}C$ ones (Figs. 3, S12, S13). $\delta^{13}C$ values also show a 2-yr periodicity (Fig. 3C).

The Element/Ca distribution in *L. uva* shows a comparatively flatter pattern with higher Li, Mg, B, U, Na, Sr, and Ba/Ca (Fig. 4A–E,G,I) compared to *L. neozelanica* and *G. vitreus*. Al/Ca (Fig. 4F) and Mn/Ca (Fig. 4H) show a subtle enrichment in the juvenile stage; Cd/Ca (Fig. 4J) stays invariant throughout the shell (Figs. S20, S21). There is a strong covariance between $\delta^{18}O$ and $\delta^{13}C$ values and $\delta^{18}O$ and B/Ca (Fig. S22).

Discussion

Ontogenetic trends

$\delta^{18}O$ values are stable between ~ 1 and 6 yr in temperate species, with a slight, yet variable, decrease in juvenile and mature stages (Figs. S17, S18). Low values in juvenile stages, when present, are best explained by kinetic effects during rapid growth rates (e.g., Rollion-Bard et al. 2019). Kinetic effects, however, do not explain low $\delta^{18}O$ values in mature stages (which are expected to grow more slowly); instead, they are most convincingly explained by growth being restricted to mostly temperate to warm seasons, when food is more plentiful (Curry 1982; Garbelli et al. 2022).

The bell-shaped $\delta^{13}C$ profile is in line with previous observations in temperate species (Von Allmen et al. 2010; Takayanagi et al. 2013; Takizawa et al. 2017; Romanin et al. 2018) and, similar to $\delta^{18}O$ values, may be to some extent affected by kinetic effects in the juvenile stage. Low $\delta^{13}C$ values in both juvenile and mature stages may be due to greater availability of metabolic CO_2 enriched in ^{12}C being incorporated into the calcite, as observed in mature stages of bivalves (Lorrain et al. 2004). The negative correlation between $\delta^{13}C$ and Element/Ca, particularly obvious in *G. vitreus*, implies similar controls. For instance, an increase in dissolved inorganic carbon (DIC) has been proposed to favor higher Sr/Ca and other divalent cations (Jurikova et al. 2020).

The Antarctic species shows a different trend. In both isotope profiles, a marked shift toward lower average values is recorded at ~ 12 yr (~ 23 mm-length), associated with changes in Element/Ca. This may correspond to endogenous factors related to reproduction. According to Peck et al. (1997), *L. uva* starts to reproduce after 10 yr (it starts to have gonad at 19–25.7 mm-length, Peck and Holmes 1989), which roughly corresponds to our observations. Reproductive activity in *L. uva* has a large interannual variability, and faster shell growth rates have been observed in summers following spawning (Peck et al. 1997). This may explain the decrease in $\delta^{18}O$ and $\delta^{13}C$ values, and the general increase in many Element/Ca after sexual maturity.

Microstructure does not seem to impact severely the geochemical composition of the analyzed species, as seen at the SEM (Supporting Information S3.1), with the same pattern occurring in different shell sequences: secondary plus tertiary vs. only tertiary layer. The same pattern is also found in different shell portions where the microstructure differs: in the anterior part comprising only the secondary layer as well as in the posterior part, which shows different proportions of secondary and tertiary layers. These observations are rather unexpected as the microstructure has been previously proposed as a driver of intra-shell chemical variabilities (Rollion-Bard et al. 2019) and render further investigation.

Intrannual, annual, and interannual patterns

The here proposed sclerochemical approach shows that intrannual, annual, and interannual patterns can be discerned in brachiopod shells and depend on species growth rates, which change with latitude.

Annual and intrannual patterns are discernible from $\delta^{18}O$, $\delta^{13}C$ and Element/Ca values in the faster-growing *L. neozelanica* and *G. vitreus*, in particular in their juvenile to adult stages, but not in the most mature anterior shell parts where growth toward the end of their lifetime stagnates. Intrannual patterns (around 0.5-yr periodicity, twice per year) may be due to reproductive cycles or to mid-seasons (i.e., spring and autumn recording the same temperature).

The highest temperature is generally recorded in the second part of each growth year, at least in juvenile stages, similarly to other modern species (Yamamoto et al. 2010, 2011). In *L. neozelanica*, this suggests a preference for larval setting and the start of shell secretion in summer–autumn (Lee et al. 2010), even though its reproduction is thought to be plastic (Baird et al. 2013). *Liothyrella neozelanica* does not

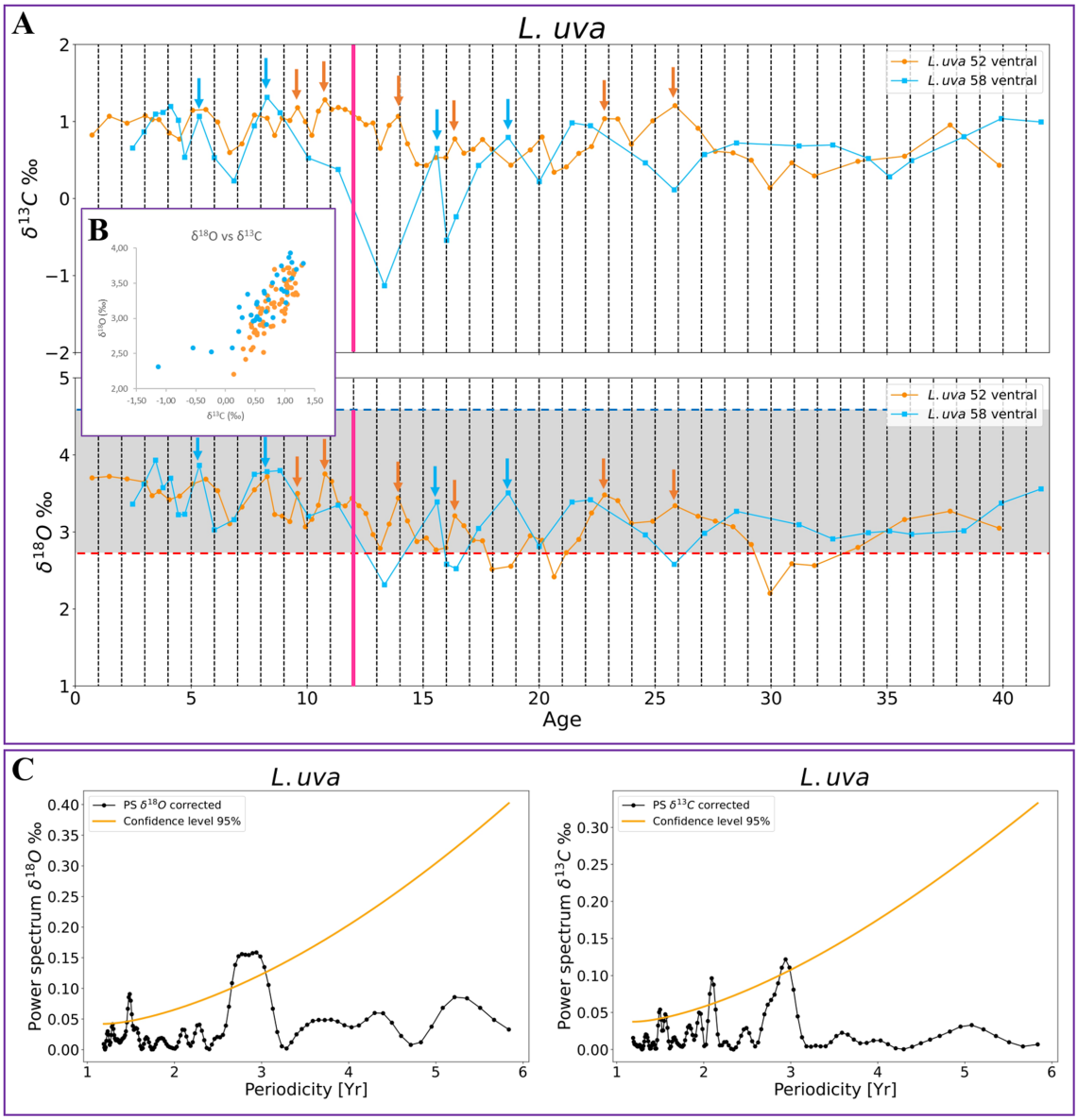

Fig. 3. (**A**) Time series of $\delta^{13}C$ and $\delta^{18}O$ data of the Antarctic species *L. uva* obtained by the Brody–Bertalanffy equation with $K = 0.036$ and $S_{\infty} = 60$ mm. The explanation of the gray horizontal box and of red and blue dotted lines is given in the caption of Fig. 2. The vertical pink line at 12 yr indicates a marked shift toward lower average values at reproduction. The arrows show some of the correspondences between $\delta^{18}O$ maxima (lower temperatures/higher salinities) in the lower panel and $\delta^{13}C$ maxima (low organic carbon oxidation) in the upper panel, for each specimen (orange arrow #52, blue arrow #58). (**B**) Cross-plots of $\delta^{18}O$ vs. $\delta^{13}C$ values showing their covariance. (**C**) Left plot: Lomb-Scargle periodogram of the isotope signal compared with the 95% confidence level curve for red noise for $\delta^{18}O$ data of *L. uva* (#52, ventral valve); significant periodicites are present around 1.5 and 3 yr. Right plot: Lomb-Scargle periodogram of the isotope signal compared with the 95% confidence level curve for red noise for $\delta^{13}C$ data of *L. uva*; significant periodicites are present around 1.5, 2, and 3 yr.

record the expected lowest and highest temperatures (Fig. 2; Table 1), as also previously reported (Romanin et al. 2018; Garbelli et al. 2022). This suggests that species sensitive to physical stresses, such as those in fjord environments (Wing and Jack 2014), stop growing when temperatures are at their extremes. *Gryphus vitreus*, although comparatively more tolerant with wide ecological preferences (Toma et al. 2022), records the periodical intrannual variation in a more stable environment, evidenced also by the very smooth Element/Ca trends.

The Antarctic *L. uva* has about five times slower annual growth rates than the temperate *L. neozelanica* and *G. vitreus* (Peck et al. 1997) and thus is potentially only useful as an archive of interannual patterns. Indeed, strong interannual

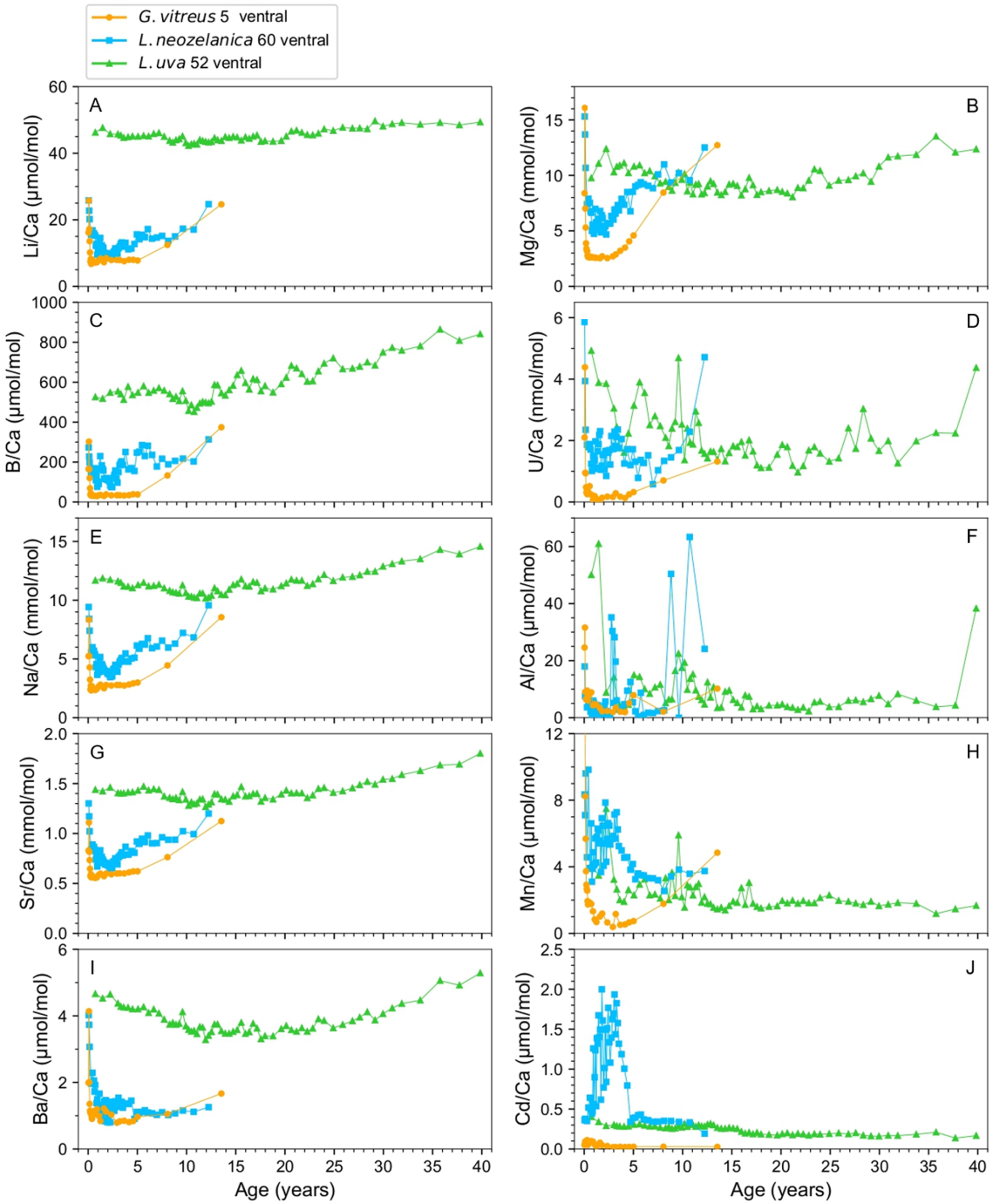

Fig. 4. Time series of Element/Ca (**A**–**J**) of ventral valves of *G. vitreus* (#5, secondary and tertiary layers sampled together), *L. neozelanica* (#60, secondary and tertiary layers sampled together), and *L. uva* (#52, only secondary layer) plotted against age (yr).

variations are recorded by both isotope profiles, positively correlated at 1.5- and 3-yr scales, with intervals of lower temperatures (and hence higher salinities) corresponding to lower organic carbon oxidation due to extended ice cover and vice versa (Marshall et al. 1997) (Fig. 3). Positively correlated to the isotope profiles is also Cd/Ca, which could be tracking the seawater [Cd] reflecting lower phytoplankton dynamics (lower phytoplankton mass under extended ice cover and higher with more ice melt). These data show that *L. uva* records the interannual variability at subdecadal scales in water mass

properties (temperature, freshwater input, and nutrients) characteristic of the Antarctic oceanic ecosystem and strongly influenced by winter sea ice changes (Clarke et al. 2008; Venables et al. 2023). Additionally, intra-shell variations in *L. uva* are also controlled by reproductive cycles as indicated by periodicity of 1.5–2 yr which fits with the data of Peck and Brey (1996) and Peck et al. (1997).

The brachiopod-based thermometer

The $\delta^{18}O$ values of *G. vitreus* and *L. neozelanica* are in the range of previously published data (Brand et al. 2019; Rollion-Bard et al. 2019), independently of the microstructure sampled (secondary fibrous or tertiary columnar or both), and correspond to the expected equilibrium field of Brand et al. (2019); equilibrium fields of Watkins et al. (2014) and Letulle et al. (2023) are shifted to higher values for *G. vitreus* (Table S3). Although still broadly within equilibrium (of Brand et al. 2019), the $\delta^{18}O$ values of *L. uva* are slightly biased toward lower values, even if the shell of this species grows seasonally and faster in winter for resource prioritization (Peck et al. 1997). The equilibrium fields of Watkins et al. (2014) and Letulle et al. (2023) are shifted to even lower values (Table S3). Marshall et al. (1997) and Parkinson et al. (2005) attributed low $\delta^{18}O$ values in *L. uva* to vital effects. The covariance between $\delta^{18}O$ and $\delta^{13}C$ values and $\delta^{18}O$ and B/Ca further supports the presence of growth-related effects in this species (Wendler et al. 2013).

Overall, our results validate and extend the application of the brachiopod-based oxygen-isotope thermometer (Brand et al. 2019) to high-resolution studies. The slow-growing Antarctic species may, however, exhibit minor biases that can be identified by combining $\delta^{18}O$ with $\delta^{13}C$ and Element/Ca data.

Author Contributions

L. Angiolini and G. Crippa: co-led the entire manuscript effort and contributed equally to the conceptualization, investigation, data analyses, and funding acquisition; M. Viaretti: contributed to the investigation and figure creation; E. M. Harper: contributed with specimen provision; M. J. Leng and K. Savickaite: contributed with stable isotope analyses; H. Jurikova and J. W. B. Rae: contributed with trace element analyses; M. Zanchi: contributed with growth, statistical, and periodicity analyses and figure creation. E. M. Harper, M. J. Leng, and H. Jurikova contributed to the review and editing of the manuscript; L. Angiolini and G. Crippa wrote the manuscript.

Acknowledgments

Two anonymous reviewers, as well as the Editor and the Associate Editor of the Special Volume, are warmly thanked for their useful and constructive comments on the manuscript. G. Crippa, L. Angiolini, and M. Viaretti acknowledge funding by the MURST PRIN 2017RX9XXXY, project "Biota resilience to global change: biomineralization of planktic and benthic calcifiers in the past, present and future" to E. Erba and by the European Union—Next Generation EU PRIN MUR 2022WEZR44 to C. Bottini. The work was also partly supported by the Italian Ministry for Universities and Research (MUR) through the project "Dipartimenti di Eccellenza 2023-27" (G. Crippa, L. Angiolini, and M. Viaretti). H. Jurikova acknowledges funding from the Leverhulme Trust Early Career Fellowship (ECF-2023-199). H. Jurikova and J. W. B. Rae acknowledge funding from the European Research Council under the European Union's Horizon 2020 research and innovation program (grant agreement 805246).

Conflicts of Interest

None declared.

References

Angiolini, L., G. Crippa, K. Azmy, et al. 2019. "The Giants of the Phylum Brachiopoda: A Matter of Diet?" *Palaeontology* 62, no. 6: 889–917. https://doi.org/10.1111/pala.12433.

Angiolini, L., F. Jadoul, M. J. Leng, et al. 2009. "How Cold Were the Early Permian Glacial Tropics? Testing Sea-Surface Temperature Using the Oxygen Isotope Composition of Rigorously Screened Brachiopod Shells." *Journal of the Geological Society* 166, no. 5: 933–945. https://doi.org/10.1144/0016-76492008-096R.

Angiolini, L., M. Stephenson, M. J. Leng, et al. 2012. "Heterogeneity, Cyclicity and Diagenesis in a Mississippian Brachiopod Shell of Palaeoequatorial Britain." *Terra Nova* 24, no. 1: 16–26. https://doi.org/10.1111/j.1365-3121.2011.01032.x.

Baird, M. J., D. E. Lee, and M. D. Lamare. 2013. "Reproduction and Growth of the Terebratulid Brachiopod *Liothyrella neozelanica* Thomson, 1918 From Doubtful Sound, New Zealand." *Biological Bulletin* 225, no. 3: 125–136. https://doi.org/10.1086/BBLv225n3p125.

Bajnai, D., J. Fiebig, A. Tomašových, et al. 2018. "Assessing Kinetic Fractionation in Brachiopod Calcite Using Clumped Isotopes." *Scientific Reports* 8: 533. https://doi.org/10.1038/s41598-017-17353-7.

Benigni, C. 1985. "Morfologia ed ultrastruttura di "*Gryphus vitreus*" (Born, 1778) dell'Arcipelago Toscano (Italia)." *Bollettino del Museo Regionale di Scienze Naturali Torino* 3: 449–498.

Brand, U., K. Azmy, M. A. Bitner, et al. 2013. "Oxygen Isotopes and $MgCO_3$ in Brachiopod Calcite and a New Paleotemperature Equation." *Chemical Geology* 359: 23–31. https://doi.org/10.1016/j.chemgeo.2013.09.014.

Brand, U., K. Azmy, E. Griesshaber, et al. 2015. "Carbon Isotope Composition in Modern Brachiopod Calcite: A Case of Equilibrium With Seawater?" *Chemical Geology* 411: 81–96. https://doi.org/10.1016/j.chemgeo.2015.06.021.

Brand, U., M. A. Bitner, A. Logan, et al. 2019. "Brachiopod-Based Oxygen-Isotope Thermometer: Update and Review." *Rivista Italiana di Paleontologia e Stratigrafia* 125, no. 3: 775–778. https://doi.org/10.13130/2039-4942/12226.

Brand, U., A. Logan, M. A. Bitner, E. Griesshaber, K. Azmy, and D. Buhl. 2011. "What Is the Ideal Proxy of Palaeozoic Seawater Chemistry?" *Memoirs of the Association of Australasian Palaeontologists* 41: 9–24. https://doi.org/10.3316/informit.637671470793265.

Brey, T., L. S. Peck, J. Gutt, S. Hain, and W. E. Arntz. 1995. "Population Dynamics of *Magellania fragilis*, a Brachiopod Dominating a Mixed-Bottom Macrobenthic Assemblage on the Antarctic Shelf." *Journal of the Marine Biological Association of the United Kingdom* 75, no. 4: 857–869. https://doi.org/10.1017/S0025315400038200.

Butler, S., T. R. Bailey, C. H. Lear, G. B. Curry, L. Cherns, and I. McDonald. 2015. "The Mg/Ca–Temperature Relationship in Brachiopod Shells: Calibrating a Potential Palaeoseasonality Proxy." *Chemical Geology* 397: 106–117. https://doi.org/10.1016/j.chemgeo.2015.01.009.

Carpenter, S. J., and K. C. Lohmann. 1995. "$\delta^{18}O$ and $\delta^{13}C$ Values of Modern Brachiopod Shells." *Geochimica et Cosmochimica Acta* 59, no. 18: 3749–3764. https://doi.org/10.1016/0016-7037(95)00291-7.

Casella, L. A., E. Griesshaber, M. Simonet-Roda, et al. 2018. "Micro-and Nanostructures Reflect the Degree of Diagenetic Alteration in Modern and Fossil Brachiopod Shell Calcite: A Multi-Analytical Screening Approach (CL, FE-SEM, AFM, EBSD)." *Palaeogeography Palaeoclimatology Palaeoecology* 502: 13–30. https://doi.org/10.1016/j.palaeo.2018.03.011.

Clark, J. V., A. Pérez-Huerta, D. P. Gillikin, A. E. Aldridge, M. Reolid, and K. Endo. 2016. "Determination of Palaeoseasonality of Fossil Brachiopods Using Shell Spiral Deviations and Chemical Proxies." *Palaeoworld* 25, no. 4: 662–674. https://doi.org/10.1016/j.palwor.2016.05.010.

Clarke, A., M. P. Meredith, M. I. Wallace, M. A. Brandon, and D. N. Thomas. 2008. "Seasonal and Interannual Variability in Temperature, Chlorophyll and Macronutrients in Northern Marguerite Bay, Antarctica." *Deep Sea Research, Part II* 55, no. 18–19: 1988–2006. https://doi.org/10.1016/j.dsr2.2008.04.035.

Crippa, G., F. Ye, C. Malinverno, and A. Rizzi. 2016. "Which Is the Best Method to Prepare Invertebrate Shells for SEM Analysis? Testing Different Techniques on Recent and Fossil Brachiopods." *Bollettino della Societàa Paleontologica Italiana* 55, no. 2: 112. https://doi.org/10.4435/BSPI.2016.11.

Cross, E. L., L. S. Peck, and E. M. Harper. 2015. "Ocean Acidification Does Not Impact Shell Growth or Repair of the Antarctic Brachiopod *Liothyrella uva* (Broderip, 1833)." *Journal of Experimental Marine Biology and Ecology* 462: 29–35. https://doi.org/10.1016/j.jembe.2014.10.013.

Curry, G. B. 1982. "Ecology and Population Structure of the Recent Brachiopod *Terebratulina* From Scotland." *Palaeontology* 25, no. 2: 227–246.

Davies, A. J., U. Brand, M. Tagliavento, et al. 2023. "Isotopic Disequilibrium in Brachiopods Disentangled With Dual Clumped Isotope Thermometry." *Geochimica et Cosmochimica Acta* 359: 135–147. https://doi.org/10.1016/j.gca.2023.08.005.

Garbelli, C., L. Angiolini, U. Brand, and F. Jadoul. 2014. "Brachiopod Fabric, Classes and Biogeochemistry: Implications for the Reconstruction and Interpretation of Seawater Carbon-Isotope Curves and Records." *Chemical Geology* 371: 60–67. https://doi.org/10.1016/j.chemgeo.2014.01.022.

Garbelli, C., L. Angiolini, R. Posenato, et al. 2022. "Isotopic Time-Series ($\delta^{13}C$ and $\delta^{18}O$) Obtained From the Columnar Layer of Permian Brachiopod Shells Are a Reliable Archive of Seasonal Variations." *Palaeogeography Palaeoclimatology Palaeoecology* 607: 111264. https://doi.org/10.1016/j.palaeo.2022.111264.

Gaspard, D. 1990. "Growth Stages in Articulate Brachiopod Shells and their Relation to Biomineralization." In *Brachiopods Through Time*, edited by D. L. MacKinnon, D. E. Lee, and J. D. Campbell, 167–174. Rotterdam: A. A. Balkema.

Gaspard, D., A. E. Aldridge, O. Boudouma, M. Fialin, N. Rividi, and C. Lécuyer. 2018. "Analysis of Growth and Form in *Aerothyris kerguelenensis* (Rhynchonelliform Brachiopod)—Shell Spiral Deviations, Microstructure, Trace Element Contents and Stable Isotope Ratios." *Chemical Geology* 483: 474–490. https://doi.org/10.1016/j.chemgeo.2018.03.018.

Griesshaber, E., R. D. Neuser, and W. W. Schmahl. 2010. "The Application of EBSD Analysis to Biomaterials: Microstructural and Crystallographic Texture Variations in Marine Carbonate Shells." *Seminario Sociedad Española de Mineralogia* 7: 22–34.

Gröcke, D. R., and D. P. Gillikin. 2008. "Advances in Mollusc Sclerochronology and Sclerochemistry: Tools for Understanding Climate and Environment." *Geo-Marine Letters* 28: 265–268. https://doi.org/10.1007/s00367-008-0108-4.

Grossman, E. L., H. S. Mii, C. Zhang, and T. E. Yancey. 1996. "Chemical Variation in Pennsylvanian Brachiopod Shells; Diagenetic, Taxonomic, Microstructural, and Seasonal Effects." *Journal of Sedimentary Research* 66, no. 5: 1011–1022. https://doi.org/10.1306/D4268469-2B26-11D7-8648000102C1865D.

Hiller, N. 1988. "The Development of Growth Lines on Articulate Brachiopods." *Lethaia* 21, no. 2: 177–188. https://doi.org/10.1111/j.1502-3931.1988.tb02069.x.

Jurikova, H., M. Ippach, V. Liebetrau, et al. 2020. "Incorporation of Minor and Trace Elements into Cultured Brachiopods: Implications for Proxy Application With New Insights From a Biomineralisation Model." *Geochimica et Cosmochimica Acta* 286: 418–440. https://doi.org/10.1016/j.gca.2020.07.026.

Jurikova, H., V. Liebetrau, M. Gutjahr, et al. 2019. "Boron Isotope Systematics of Cultured Brachiopods: Response to Acidification, Vital Effects and Implications for Palaeo-pH

Reconstruction." *Geochimica et Cosmochimica Acta* 248: 370–386. https://doi.org/10.1016/j.gca.2019.01.015.

Kocsis, L., A. Dulai, A. Cipriani, T. Vennemann, and M. Yunsi. 2020. "Geochemistry of Recent and Fossil Brachiopod Calcite of *Megathiris detruncata* (Terebratulida, Megathyrididae): A Modern Baseline Study to Trace Past Environmental Conditions." *Chemical Geology* 533: 119335. https://doi.org/10.1016/j.chemgeo.2019.119335.

Lee, D. E., J. H. Robinson, J. D. Witman, et al. 2010. "Observations on Recruitment, Growth and Ecology in a Diverse Living Brachiopod Community, Doubtful Sound, Fiordland, New Zealand." *Special Papers in Palaeontology* 84: 177–191. https://doi.org/10.1111/j.1475-4983.2010.00996.x.

Letulle, T., D. Gaspard, M. Daëron, et al. 2023. "Multi-Proxy Assessment of Brachiopod Shell Calcite as a Potential Archive of Seawater Temperature and Oxygen Isotope Composition." *Biogeosciences* 20, no. 7: 1381–1403. https://doi.org/10.5194/bg-20-1381-2023.

Lomb, N. R. 1976. "Least-Squares Frequency Analysis of Unequally Spaced Data." *Astrophysics and Space Science* 39: 447–462. https://doi.org/10.1007/BF00648343.

Lorrain, A., Y. M. Paulet, L. Chauvaud, R. Dunbar, D. Mucciarone, and M. Fontugne. 2004. "$\delta^{13}C$ Variation in Scallop Shells: Increasing Metabolic Carbon Contribution With Body Size?" *Geochimica et Cosmochimica Acta* 68, no. 17: 3509–3519. https://doi.org/10.1016/j.gca.2004.01.025.

Lowenstam, H. A. 1961. "Mineralogy, O^{18}/O^{16} Ratios, and Strontium and Magnesium Contents of Recent and Fossil Brachiopods and their Bearing on the History of the Oceans." *Journal of Geology* 69, no. 3: 241–260. https://doi.org/10.1086/626740.

Marshall, J. D., D. Pirrie, A. Clarke, C. P. Nolan, and J. Sharman. 1997. "Stable-Isotopic Composition of Skeletal Carbonates From Living Antarctic Marine Invertebrates." *Lethaia* 29, no. 2: 203–212. https://doi.org/10.1111/j.1502-3931.1996.tb01877.x.

McKinnon, D. I. 1974. "The Shell Structure of Spiriferid Brachiopoda." *British Museum Bulletin* 25, no. 3: 187–261.

Mii, H. S., and E. L. Grossman. 1994. "Late Pennsylvanian Seasonality Reflected in the ^{18}O and Elemental Composition of a Brachiopod Shell." *Geology* 22, no. 7: 661–664. https://doi.org/10.1130/0091-7613(1994)022%3C0661:LPSRIT%3E2.3.CO;2.

Müller, T., A. Tomašových, M. L. Correa, R. Mertz-Kraus, and T. Mikuš. 2022. "Mapping Intrashell Variation in Mg/Ca of Brachiopods to External Growth Lines: Mg Enrichment Corresponds to Seasonal Growth Slowdown." *Chemical Geology* 593: 120758. https://doi.org/10.1016/j.chemgeo.2022.120758.

Ostrow, D. G. 2004. *Larval Dispersal and Population Genetic Structure of Brachiopods in the New Zealand Fiords*. PhD thesis, 162. University of Otago.

Parkinson, D., G. B. Curry, M. Cusack, and A. E. Fallick. 2005. "Shell Structure, Patterns and Trends of Oxygen and Carbon Stable Isotopes in Modern Brachiopod Shells." *Chemical Geology* 219, no. 1–4: 193–235. https://doi.org/10.1016/j.chemgeo.2005.02.002.

Peck, L. S., and T. Brey. 1996. "Bomb Signals in Old Antarctic Brachiopods." *Nature* 380, no. 6571: 207–208. https://doi.org/10.1038/380207b0.

Peck, L. S., S. Brockington, and T. Brey. 1997. "Growth and Metabolism in the Antarctic Brachiopod *Liothyrella uva*." *Philosophical Transactions of the Royal Society of London. Series B: Biological Sciences* 352, no. 1355: 851–858. https://doi.org/10.1098/rstb.1997.0065.

Peck, L. S., and L. J. Holmes. 1989. "Seasonal and Ontogenetic Changes in Tissue Size in the Antarctic Brachiopod *Liothyrella uva* (Broderip, 1833)." *Journal of Experimental Marine Biology and Ecology* 134, no. 1: 25–36. https://doi.org/10.1016/0022-0981(90)90054-G.

Pierre, C. 1999. "The Oxygen and Carbon Isotope Distribution in the Mediterranean Water Masses." *Marine Geology* 153, no. 1–4: 41–55. https://doi.org/10.1016/S0025-3227(98)00090-5.

Popp, B. N., T. F. Anderson, and P. A. Sandberg. 1986. "Brachiopods as Indicators of Original Isotopic Compositions in Some Paleozoic Limestones." *Geological Society of America Bulletin* 97, no. 10: 1262–1269. https://doi.org/10.1130/0016-7606(1986)97%3C1262:BAIOOI%3E2.0.CO;2.

Roark, A., E. L. Grossman, and J. Lebold. 2016. "Low Seasonality in Central Equatorial Pangea during a Late Carboniferous Highstand Based on High-Resolution Isotopic Records of Brachiopod Shells." *Geological Society of America Bulletin* 128, no. 5–6: 1056. https://doi.org/10.1130/B31330.1.

Rollion-Bard, C., S. M. Garcia, P. Burckel, et al. 2019. "Assessing the Biomineralization Processes in the Shell Layers of Modern Brachiopods From Oxygen Isotopic Composition and Elemental Ratios: Implications for their Use as Paleoenvironmental Proxies." *Chemical Geology* 524: 49–66. https://doi.org/10.1016/j.chemgeo.2019.05.031.

Rollion-Bard, C., H. Jurikova, and D. Henkel. 2024. "High-Resolution Carbon and Oxygen Isotopic Compositions of Cultured Brachiopods: Effect of pH, Temperature and Growth." *Chemical Geology* 659: 1222132. https://doi.org/10.1016/j.chemgeo.2024.122132.

Romanin, M., G. Crippa, F. Ye, et al. 2018. "A Sampling Strategy for Recent and Fossil Brachiopods: Selecting the Optimal Shell Segment for Geochemical Analyses." *Rivista Italiana di Paleontologia e Stratigrafia* 124, no. 2: 343–359. https://doi.org/10.13130/2039-4942/10193.

Rudwick, M. J. 1962. "Filter-Feeding Mechanisms in some Brachiopods From New Zealand." *Journal of the Linnean Society of London, Zoology* 44, no. 300: 592–615. https://doi.org/10.1111/j.1096-3642.1962.tb01626.x.

Scargle, J. D. 1982. "Studies in Astronomical Time Series Analysis. II—Statistical Aspects of Spectral Analysis of Unevenly Spaced Data." *Astrophysical Journal* 263, no. 1: 835–853. https://doi.org/10.1086/160554.

Schmahl, W. W., E. Griesshaber, K. Kelm, et al. 2012. "Hierarchical Structure of Marine Shell Biomaterials:

Biomechanical Functionalization of Calcite by Brachiopods." *Zeitschrift fur Kristallographie—Crystalline Materials* 227, no. 11: 793–804. https://doi.org/10.1524/zkri.2012.1542.

Schmahl, W. W., E. Griesshaber, R. Neuser, A. Lenze, R. Job, and U. Brand. 2004. "The Microstructure of the Fibrous Layer of Terebratulide Brachiopod Shell Calcite." *European Journal of Mineralogy* 16, no. 4: 693–697. https://doi.org/10.1127/0935-1221/2004/0016-0693.

Schulz, M., and M. Mudelsee. 2002. "REDFIT: Estimating Red-Noise Spectra Directly From Unevenly Spaced Paleoclimatic Time Series." *Computational Geosciences* 28, no. 3: 421–426. https://doi.org/10.1016/S0098-3004(01)00044-9.

Schumann, D. 2011. "Growth Rates of *Calloria inconspicua* (Sowerby, 1846) From the Upper Intertidal Zone of Portobello, New Zealand." *Memoirs of the Association of Australasian Palaeontologists* 41: 39–44.

Simonet Roda, M., E. Griesshaber, A. Ziegler, et al. 2019. "Calcite Fibre Formation in Modern Brachiopod Shells." *Scientific Reports* 9, no. 1: 598. https://doi.org/10.1038/s41598-018-36959-z.

Takayanagi, H., R. Asami, O. Abe, H. Kitagawa, T. Miyajima, and Y. Iryu. 2012. "Carbon- and Oxygen-Isotope Compositions of a Modern Deep-Water Brachiopod *Campagea japonica* Collected off Aguni-Jima, Central Ryukyu Islands, Southwestern Japan." *Geochemical Journal* 46, no. 2: 77–87. https://doi.org/10.2343/geochemj.1.0153.

Takayanagi, H., R. Asami, O. Abe, et al. 2013. "Intraspecific Variations in Carbon-Isotope and Oxygen-Isotope Compositions of a Brachiopod *Basiliola lucida* Collected off Okinawa-Jima, Southwestern Japan." *Geochimica et Cosmochimica Acta* 115: 115–136. https://doi.org/10.1016/j.gca.2013.03.026.

Takayanagi, H., R. Asami, T. Otake, et al. 2015. "Quantitative Analysis of Intraspecific Variations in the Carbon and Oxygen Isotope Compositions of the Modern Cool-Temperate Brachiopod *Terebratulina crossei*." *Geochimica et Cosmochimica Acta* 170: 301–320. https://doi.org/10.1016/j.gca.2015.08.006.

Takizawa, M., H. Takayanagi, K. Yamamoto, O. Abe, K. Sasaki, and Y. Iryu. 2017. "Paleoceanographic Conditions at Approximately 20 and 70 Ka Recorded in *Kikaithyris hanzawai* (Brachiopoda) Shells." *Geochimica et Cosmochimica Acta* 215: 189–213. https://doi.org/10.1016/j.gca.2017.08.002.

The Astropy Collaboration, and 137 coathors. 2022. "The Astropy Project: Sustaining and Growing a Community-Oriented Open-Source Project and the Latest Major Release (v5. 0) of the Core Package." *Astrophysical Journal* 935, no. 2: 167. https://doi.org/10.3847/1538-4357/ac7c74.

Toma, M., F. Enrichetti, G. Bavestrello, et al. 2022. "Brachiopod Fauna From the Deep Mediterranean Sea: Distribution Patterns and Ecological Preferences." *Diversity* 14, no. 9: 753. https://doi.org/10.3390/d14090753.

Ullmann, C. V., R. Frei, C. Korte, and C. Lüter. 2017. "Element/Ca, C and O Isotope Ratios in Modern Brachiopods: Species-Specific Signals of Biomineralization." *Chemical Geology* 460: 15–24. https://doi.org/10.1016/j.chemgeo.2017.03.034.

Veizer, J., D. Ala, K. Azmy, et al. 1999. "$^{87}Sr/^{86}Sr$, $\delta^{13}C$ and $\delta^{18}O$ Evolution of Phanerozoic Seawater." *Chemical Geology* 161, no. 1–3: 59–88. https://doi.org/10.1016/S0009-2541(99)00081-9.

Venables, H., M. P. Meredith, K. R. Hendry, et al. 2023. "Sustained Year-Round Oceanographic Measurements From Rothera Research Station, Antarctica, 1997–2017." *Scientific Data* 10, no. 1: 265. https://doi.org/10.1038/s41597-023-02172-5.

Von Allmen, K., T. F. Nägler, T. Pettke, et al. 2010. "Stable Isotope Profiles (Ca, O, C) through Modern Brachiopod Shells of *T. septentrionalis* and *G. vitreus*: Implications for Calcium Isotope Paleo-Ocean Chemistry." *Chemical Geology* 269, no. 3–4: 210–219. https://doi.org/10.1016/j.chemgeo.2009.09.019.

Watkins, J. M., J. D. Hunt, F. J. Ryerson, and D. J. DePaolo. 2014. "The Influence of Temperature, pH, and Growth Rate on the $\delta^{18}O$ Composition of Inorganically Precipitated Calcite." *Earth and Planetary Science Letters* 404: 332–343. https://doi.org/10.1016/j.epsl.2014.07.036.

Wendler, I., B. T. Huber, K. G. MacLeod, and J. E. Wendler. 2013. "Stable Oxygen and Carbon Isotope Systematics of Exquisitely Preserved Turonian Foraminifera From Tanzania—Understanding Isotopic Signatures in Fossils." *Marine Micropaleontology* 102: 1–33. https://doi.org/10.1016/j.marmicro.2013.04.003.

Williams, A. 1968. "A History of Skeletal Secretion Among Articulate Brachiopods." *Lethaia* 1, no. 3: 268–287. https://doi.org/10.1111/j.1502-3931.1968.tb01741.x.

Williams, A., C. H. C. Brunton, and D. I. MacKinnon. 1997. "Morphology." In *Treatise on Invertebrate Palaeontology (Part H, Brachiopoda Revised)*, edited by R. L. Kaesler, 321–422. Boulder, CO: Geological Society of America—University of Kansas Press.

Williams, A., and M. Cusack. 2007. "Chemicostructural Diversity of the Brachiopod Shell." In *Treatise on Invertebrate Paleontology. Part H. Brachiopoda (Revised) 6*, edited by P. A. Selden, 2396–2521. Boulder, CO: Geological Society of America—University of Kansas Press.

Wing, S. R., and L. Jack. 2014. "Fiordland: the ecological basis for ecosystem management." *New Zealand Journal of Marine and Freshwater Research* 48: 577–593. https://doi.org/10.1080/00288330.2014.897636

Yamamoto, K., R. Asami, and Y. Iryu. 2010. "Carbon and Oxygen Isotopic Compositions of Modern Brachiopod Shells From a Warm-Temperate Shelf Environment, Sagami Bay, Central Japan." *Palaeogeography Palaeoclimatology Palaeoecology* 291, no. 3–4: 348–359. https://doi.org/10.1016/j.palaeo.2010.03.006.

Yamamoto, K., R. Asami, and Y. Iryu. 2011. "Brachiopod Taxa and Shell Portions Reliably Recording Past Ocean Environments: Toward Establishing a Robust Paleoceanographic

Proxy." *Geophysical Research Letters* 38: L13601. https://doi.org/10.1029/2011GL047134.

Ye, F., G. Crippa, L. Angiolini, et al. 2018. "Mapping of Recent Brachiopod Microstructure: A Tool for Environmental Studies." *Journal of Structural Biology* 201: 221–236. https://doi.org/10.1016/j.jsb.2017.11.011.

Ye, F., C. Garbelli, S. Shen, and L. Angiolini. 2020. "The Shell Fabric of Palaeozoic Brachiopods: Patterns and Trends." *Lethaia* 54, no. 3: 419–439. https://doi.org/10.1111/let.12412.

Supporting Information

Additional Supporting Information may be found in the online version of this article.

Submitted 16 April 2024
Revised 10 February 2025
Accepted 16 February 2025